Improve the Stilling Basin Downstream Radial Gates

Gamal H. Elsaeed[1], Abdelazim M. Ali[2], Neveen B. Abdelmageed[1]

[1]Department of Civil Engineering, Faculty of Engineering, Shobra, Banha University, Cairo, Egypt
[2]Hydraulics Research Institute, National Water Research Center, Cairo, Egypt

Abstract In this study, the effect of positive step located at the end of the stilling basin (end step) and baffle block on the flow characteristics downstream the radial gate of the Assuit Barrages physical model was investigated. These characteristics include the main parameters of the submerged hydraulic jump, the vertical velocity distribution along the bed, the velocity decay, and the stability of bed protection downstream the apron of the stilling basin. Three different shapes of the end step and five different shapes of baffle block were tested. The physical model was built at the Hydraulics Research Institute, Delta Barrage, Egypt. The used flume has 1.0 m wide, 26.0 m long and 1.20 m deep. The flume side walls are made of glass with steel-frames to allow visual investigation of the flow patterns and stability of bed protection. Different designs of sluiceway stilling basin are examined to obtain a near optimum stilling basin design which gives the best velocity distribution along the stilling basin, minimum velocity near the bed, minimum scouring potential, the shortest length of submerged hydraulic jump, efficient energy dissipation, study characteristics submerged hydraulic jump and the stability of river bed protection. The study carries out in case submerged hydraulic jump takes place downstream the gate.

Keywords Stilling Basin, Hydraulic Jump, Assuit Barrages, Radial Gates

1. Introduction

The Ministry of Water Resources and Irrigation (MWRI), has implemented various structures and facilities along the Nile River to release water in accordance with man's requirements and needs. Various barrages have been built a on the Nile River in order to regulate water distribution and control flows to maximize profitability and minimize losses, such as Esna, and Naga Hammadi Barrages. During the testing of New Esna Barrage design and performance on a physical model, it was observed that the scour immediately downstream the stilling basin exceeded the expected values. This observation has been verified further during the monitoring of the actual structure. The same findings were also observed during the design and model testing of New Naga Hammadi Barrage. In both cases significant design modifications has been introduced using trial and error based on expert's opinion. Therefore, there is a need to develop and improve some design criteria for hydraulic structures to be used in future applications and suitable for the Nile River conditions. Different shapes of stilling basins were tested in order to investigate and study the stilling basins with the submerged hydraulic jump. The investigation included the characteristics of the submerged hydraulic jump which included the length of submerged jump and the energy losses, the velocity distribution and the velocity near bed along the stilling basin and the stability of bed protection downstream the apron as well. [1] studied the characteristics of the velocity distribution in a hydraulic jump stilling basin with five parallel offset jets in a twin-layer configuration. [2] studied stilling basin with a block ramp, which is a peculiar stream restoration structure. [3] developed the efficient stilling basins for pipe outlets. [4] studied experimentally the effect of using different spaced corrugated aprons on the downstream local scour due to submerged jump. [5] studied experimentally the effect of using line of floor water jets on Minimizing scour downstream of hydraulic structures. [6] stuided the scour

downstream hydraulic structures using semi-circular sill. They found that the semicircular sill decreased the scour hole dimensions and increased the hydraulic jump efficiency. [7] studied experimentally the effect of using three lines of angle baffles on scour downstream a control structure. And concluded that, in general, using the suggested baffle system adjacent to the weir body minimizes the deformed scour depth. Once again, decreasing Froude number leads to move the position of maximum scour depth towards the floor end. [8] studied experimentally double line angle baffles to minimize the deformed scour holes downstream hydraulic structures. [9] investigated experimentally the free rectangular hydraulic jump phenomenon on rough channel bed with dentated, solid, zigzagged bed sills, under different flow conditions using different bed sill heights and different bed sill locations. [10] conducted an experimental study using a single line of angle baffles. An angle shape baffle with vertical faces was suggested to be used as an additional element to the existing structures to minimize the impacts of excessive severe scouring downstream water structures. [11] investigated experimentally the effect of flow and sill parameters on the discharge coefficient on a vertical gate downstream of a radial basin containing lateral sill. The coefficient of discharge was increased as the sill moved downstream the gate and attain maximum value at 0.75 of the basin length. [12] studied experimentally the openings fixed in the body of weirs. Three cases of opening arrangements were included: no opening, one opening, and three openings. Empirical formula was developed for estimating scour hole depth in terms of downstream of flow conditions, Froude number, height of the weir, number of openings, area of openings, and diameters and heights of the openings. [13] studied expermentally the effect of end step shape in the performance of stilling basins downstream radial gates. [14] used different intermiade sill to improve the stilling basin sill to decrase the hydrulic jump length.

This research will focus on study optimum stilling basin gives high energy dissipation and more riprap stability downstream stilling basin. Which stilling basins consider one energy disspators should be provided at the foot of hydraulic structures for dissipating the excessive kinetic energy.

2. The Experimental Work
2.1. Model Description

Figure 1: General View of the Flume

All of the experiments were conducted in a flume located in the Hydraulics Research Institute experimental hall of the National Water Research Center, Egypt. The flume was 1.0m wide, 26.0m long and 1.20m deep flume, Fig. (1). The side walls along the entire length of the flume were made of glass with steel- frames, to allow visual investigation of the flow patterns and stability of bed protection. The flume bed was made of concrete and provided with a steel pipe to drain the water from the flume. The tail water depth was controlled by a tailgate located at flume end. The flume inlet was consisted of a masonry basin of 3.0m width, 3.0m length and 2.5m depth. The flume exit was consisted of a basin started directly by the end of the simulated reach followed by steel flap gate. The tailgate was hinged at the bottom to provide an adjustable inclination, to control the downstream tail water depth. An electro-magnetic flow meter was installed on a feeder pipe of 10 inch diameter to measure the discharge. The water discharged into the flume through two pumps with different capacities; 150,

and 500l/s. The pumps were connected to two pipelines 16 and 10 inches, respectively. The maximum feeding capacity of the system was 650 l/s. This capacity was sufficient enough for all required tests.

2.2. Model Construction
2.2.1. The sluiceway and apron
A sluiceway bay was constructed at a distance of about 10.7m downstream flume inlet The sluiceway bay consisted of a gated sill and two half-piers (9.5cm thick each) symmetrically installed on both wall sides. A bras radial gate with a radius of 57cm was used to regulate the flow. A rubber strip was fixed and compressed at both flume sides to assure no leakage from the flume sides. The radial gate is rested on a raised sill with a length of 0.49m and width of 0.81m followed by an inclined apron of 1.97m length with different slopes. A horizontal apron of 1.61m length started from the end point of the inclined apron to the downstream side, Fig. (2).
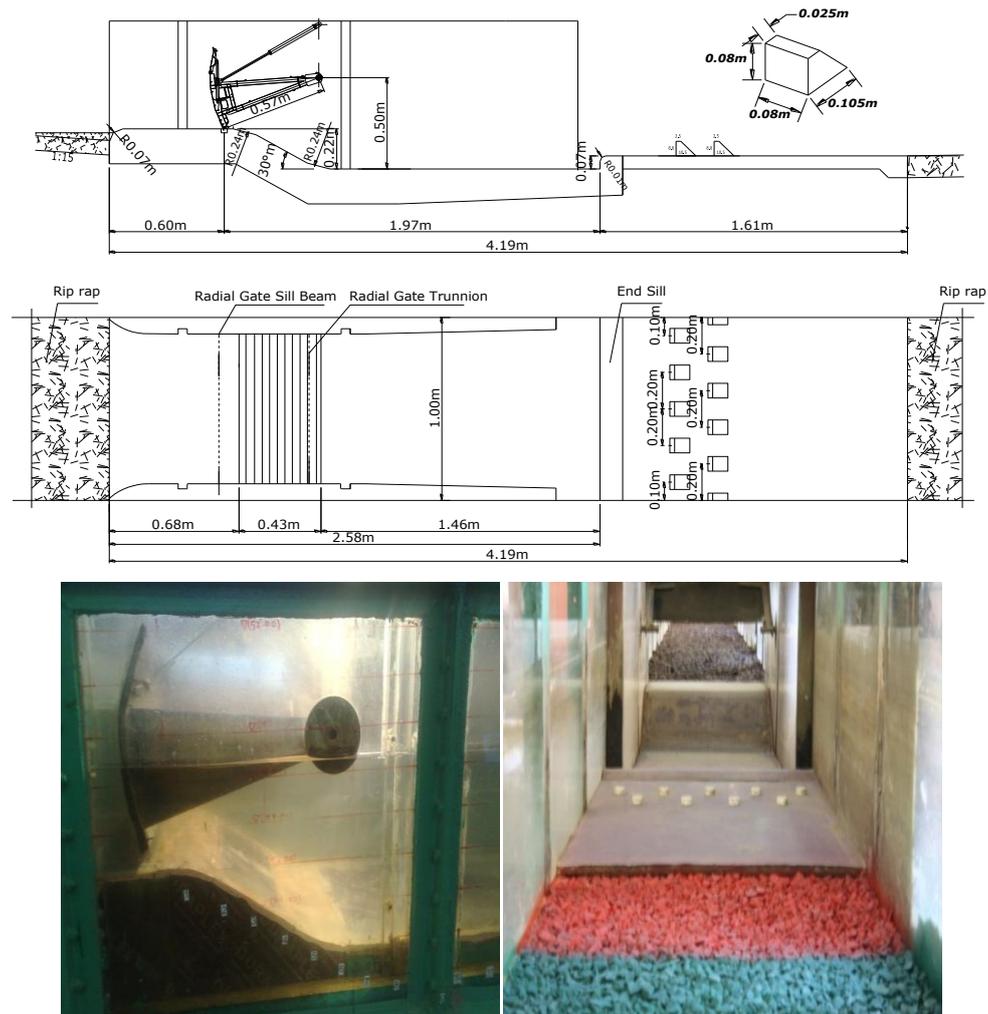
Figure 2: Geometry of Sluiceway and Apron

2.2.2. The bed material
The flume bed was consisted of two movable bed materials, sand as a foundation layer and covered by riprap in specific locations. The d_{50} of the used sand and riprap were 0.463 and 26.23mm, respectively. The sand was covered by the riprap at the first 10.3m upstream the stilling basin and the first 9.3m downstream it.

2.2.3. Measuring devices
These measuring devices in the current study were flow meter, current meter, and point gauge. Both flow meter and current meter were from electromagnetic type. The flow meter has ±1% accuracy, used for measuring the flow discharge. The current meter has ±2% accuracy, used for measuring the flow velocity. The point gauge has ±0.1mm accuracy, used for adjusting the water level at the upstream and downstream gates.

2.2.4. Model runs

Nine design shapes of stilling basins were tested in order to investigate and study the stilling basins with the submerged hydraulic jump. The investigation included the flow condition along the stilling basin, stability of bed protection downstream the apron, the length of reverse flow downstream end step, and the characteristics of the submerged hydraulic jump as well. The total number of the suggested designs used in this study was seven. Table (1) is used to define the geometric variables for each test series. Several runs are executed for each design using six different flow conditions for every test series. Fig. (3) illustrates the geometry of stilling basin and baffle blocks.

2.2.5. Test series description:

In this section a detailed description for each group will be given in order to know the differences between each group. Nine different designs (A, B, C, D, E, F, G, H, and I) for the stilling basin investigation under four groups were studied. The first group had stepped with sharp edges. The second group had additional step. The third group was without additional step and the existing one had rounded edges with different radii. The fourth group had rounded edge step with fixed radius and different designs for roughness elements.

Table 1: Types, numbers, and dimensions of baffle blocks

Case No.	End step shap		Roughness shap		Number of roughness row
A	sharp edge		Without		
B	sharp edge		Cylinder with 2cm in heght and 4cm in radius		2
C	sharp edge with additional step		Without		
D	sharp edge with additional step		Cylinder with 2cm in heght and 4cm in radius		2
E	rounded with radius 1cm		Without		
F	rounded with radius 1.7cm		Without		
G	rounded with radius 1cm		Trapzoidal with slope 4:5.5		2
H	rounded with radius 1cm		Trapzoidal with slope 1:1		2
I	rounded with radius 1cm		Trapzoidal with slope 3:4		7

Figure 3: Geometry of Stilling Basin and Baffle Blocks

2.2.6. Hydraulic variables

The hydraulic variables were designed in such a way to cover a wide range of barrages along the Nile River such as New Esna Barrage, New Naga Hammadi Barrage, Assuit Barrage, Delta Barrage, Zifta and Idfina Barrages. The main hydraulic variables were; the discharge, differential head and the downstream water depth. Based on the prototype hydraulic conditions of the different barrages on the Nile River, the hydraulic conditions for all test series were prepared. Table (2) shows the hydraulic condition for all test series that tested in this study.

Table 2: The Hydraulic Conditions for the Executed runs for All the Test Series

Test No.	Flow Discharge (Q)(Lit/s)	Upstream Water Depth (Hu) (m)	Downstream Water Depth (Yt) (m)	Differential Head (h) (m)
1	247.4	0.438	0.58	0.072
2	179.37	0.438	0.54	0.117
3	136.1	0.438	0.5	0.154
4	99	0.438	0.46	0.195
5	74.2	0.438	0.43	0.228
6	49.5	0.438	0.39	0.267
7	142.2	0.438	0.54	0.148
8	92.8	0.438	0.5	0.267
9	49.5	0.438	0.46	0.195
10	136.1	0.4	0.48	0.138
11	99	0.4	0.44	0.178
12	74.2	0.4	0.41	0.211

3. Dimensional Analysis

The hydraulic jump parameters and the energy dissipation downstream of a stilling basin with different steps variables of flow as follows:

$$\emptyset\left(c_d, Y_1, Y_2, Y_3, G.o, L_{sj}, E_1, E_2, V, g\right) = 0 \tag{1}$$

Where: C_d is the discharge coefficient, F_{r1}, is the Froude number before the hydraulic jump, y1 is the vena contracta, y_2 the sequent depth, G.O. gate opening, L_{sj} is the hydraulic jump length, E_1 is the specific energy before hydraulic jump, E_2 is the specific energy after hydraulic jump, V_1 is the mean velocity before hydraulic jump, g is gravitational acceleration. Then, the Eq. (1) might be written in the following form:

Using π-theorem and applying the properties of dimensional analysis, it yields;

$$C_d = F(\frac{V}{\sqrt{gy_1}}, \frac{y_1}{G.O}, \frac{y_3}{G.O}) \tag{2}$$

Where: C_d is the ratio between measured discharge and theoretical discharge, $\frac{V}{\sqrt{gY_1}}$ is the Froude number.

Additionally the relative hydraulic jump $\frac{L_{sj}}{Y_1}$ is related to other dimensionless parameters.

$$\frac{L_{sj}}{Y_1} = F(\frac{V}{\sqrt{gY_1}}, \frac{E_1}{E_2}, \frac{Y_1}{Y_2}) \tag{3}$$

3. Analysis and Results

The experimental results were analyzed and discussed in order to evaluate the performance of different designs of stilling basins. In the following sections the detailed analysis for the velocity measurements, the stability of bed protection material downstream the concrete slab and the characteristics of the submerged hydraulic jump were discussed. A comparison between the different designs was executed in order to study the behavior of each stilling basin with different measured parameters. Following this stage another comparison between the designs to present the optimum set results from each group were carried out in order to reach a final conclusion from this research.

4.1. Effect of Gate Opening:

Fig. (4) presents the relation between the Gate Opening and the discharge for all tested runs. The figure shows that the discharge gives a direct relationship and can be mathematically described by the following equation $Q = 9.07 * G.O + 14.77$. Figure 5 illustrates the relation between the Gate Opening and the Vena Contracta for all tested runs. From fig. (5) investigations, it can be seen that as the gate opening increases, the depth at Vena Contracta increase.
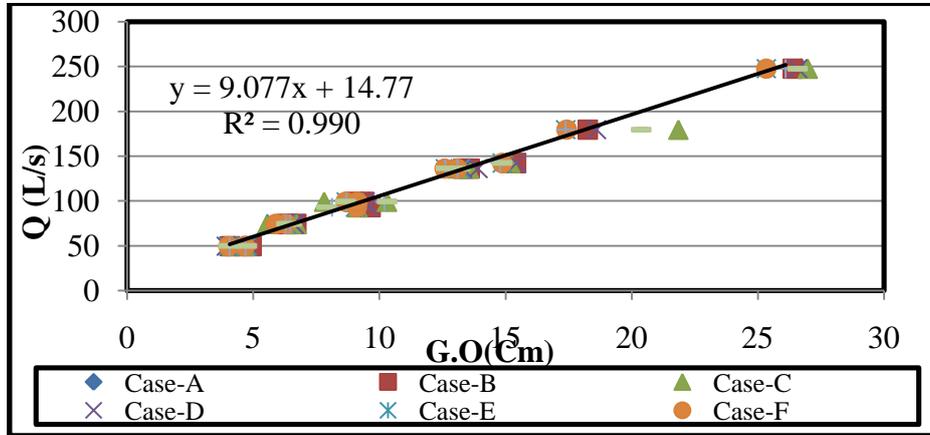
Figure 4: Relationship between Gate Opening G.O vs. Discharge Q
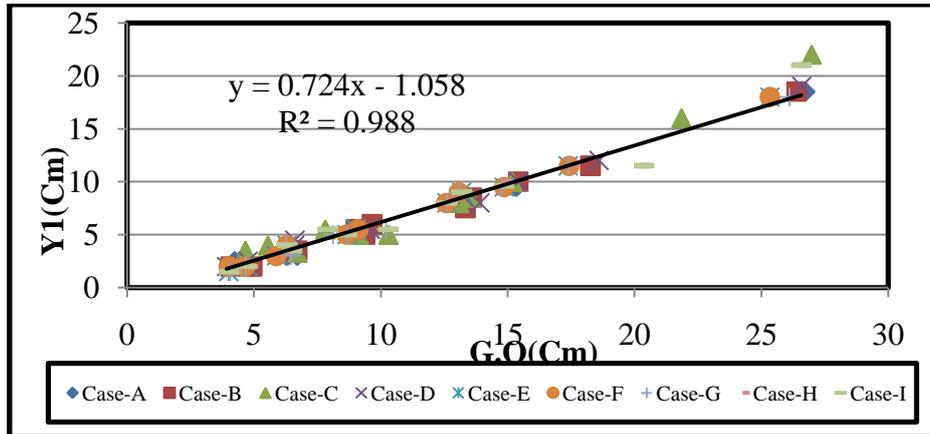
Figure 5: Relationship between Gate Opening G.O vs. Vena Contacta Y₁

The relation between Froude No. and the Vena contracta (Y1) for all cases gave the same trend and the difference between the curves is too small. So, Case-A was selected as a sample. Fig. (6) indicates the measured results compared to the corresponding obtained by Henderson (1965). The comparison showed good agreement between them. Also, the shown figure indicates the inverse relationship between the Froude no. and the depth of the Vena contracta.
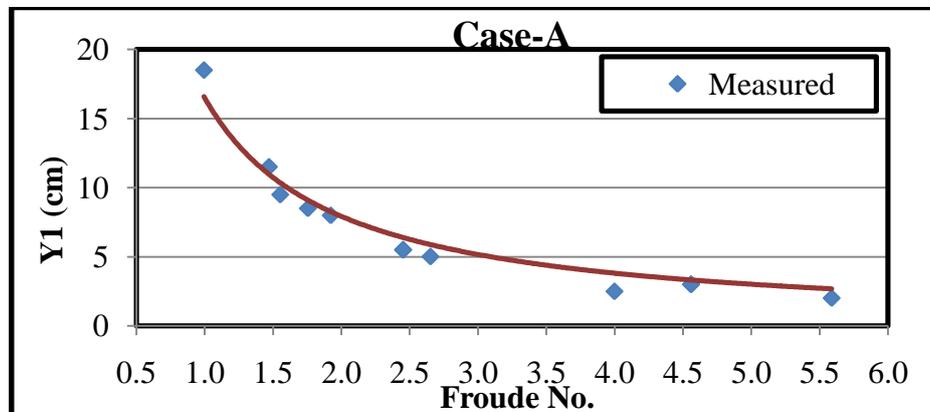
Figure 6: Relationship between Froude No. Fr and Vena contracta

Fig. (7) illustrates the relation between the relative gate opening (Y1/G.O) and the discharge coefficient for all tested runs. From figure investigations it can be seen that as the relative gate opening increases, the value of discharge coefficient decrease. The value of discharge coefficient (Cd) is varied from 1.77 to 1.2 for all tests. The figure shows that the discharge coefficient gives a parabola relationship and can be mathematically described by the following equation

$$C_d = -5.4 \left(\frac{Y_1}{G.O}\right)^4 + 83.3\left(\frac{Y_1}{G.O}\right)^3 - 116.6\left(\frac{Y_1}{G.O}\right)^2 + 54.17 \left(\frac{Y_1}{G.O}\right) - 6.6$$
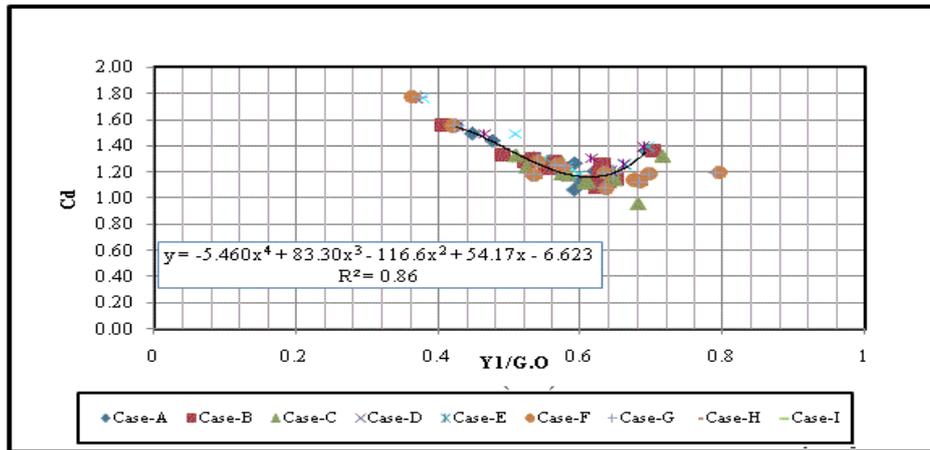
Figure 7: Relationship between relative gate opening and discharge coefficient

Multiple regression analysis was carried out with different combinations of the dimensionless parameters in Eq. (2). Several linear and nonlinear multiple regressions were conducted using the Linear and Nonlinear Regressing Package of Datafit v.9. The results for each flow condition are shown in table (3).

Table 3: Regression Analysis

No.	Equation	R^2
1	$C_d = 0.0104Y_3 + 0.0088G.O + 0.00227Y_1 + 0.12055F_{r1} + 0.573$	$R^2= 0.9$
2	$C_d = 0.0107G.O + 0.00814Y_1 + 0.1157F_{r1} + 0.75876$	$R^2= 0.75$
3	$C_d = -7E^{-6}\left(\frac{y1}{b}\right)^5 - 0.011\left(\frac{y1}{b}\right)^3 + 0.126\left(\frac{y1}{b}\right)^2 - 0.641\left(\frac{y1}{b}\right) + 2.376$	$R^2= 0.926$

Where: C_d is the discharge ceffeicent , G.O is the gate openning, Y_1 is the water depth upstream the gate, Y_3 is the water depth downstream the radial ate,and F_{r1} is the Froude number

4.2. Effect on Energy Loss

Percentage of the relative energy losses (E_L/E_1) was calculated in order to check the design efficiency of the design of spillway stilling basin. Where, E_L is energy Loss in the hydraulic jump, and E_1 is the energy at the beginning of the jump. Fig. (8) is carefully selected to investigate the influence of relative energy losses (E_L/E_1) on Froude number (F_r) for all tested cases. A direct proportional relationship was clearly noticed. For same Froude number the maximum value of the percentage of relative energy losses was found at stilling basin without roughness sill (cases A and C) and the minimum energy loss was found at case I.
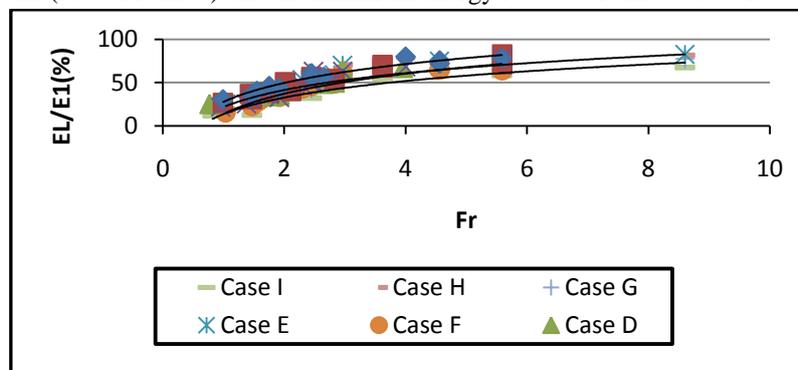
Figure 8: Relationship Between Relative Energy Losses (E_L/E_1) and Froude No. (F_r)

4.3. Effect on Sequent Depth

A Fig. (9) illustrates the influence of Froude No. (Fr) on the sequent water depth (Y_2/Y_1) associated to the hydraulic jump for the tested cases. Figure investigations emphasized that as the Froude No. increases the sequent depth increase. The maximum value of sequent depth was found at stilling basin with end step and 2 rows of rounded baffle blocks, "Q=49.5 L/s, H_u=0.438 (test D-6)

The chart shows the relationship with the fitted equation:

$$Fr = 0.014(Y_2/Y_1)^2 - 0.029(Y_2/Y_1) + 1.317$$

Legend: ◆ Case-A, ■ Case-B, ▲ Case-C, ✕ Case-D, ✳ Case-E, ● Case-F, + Case-G, – Case-H, – Case-I
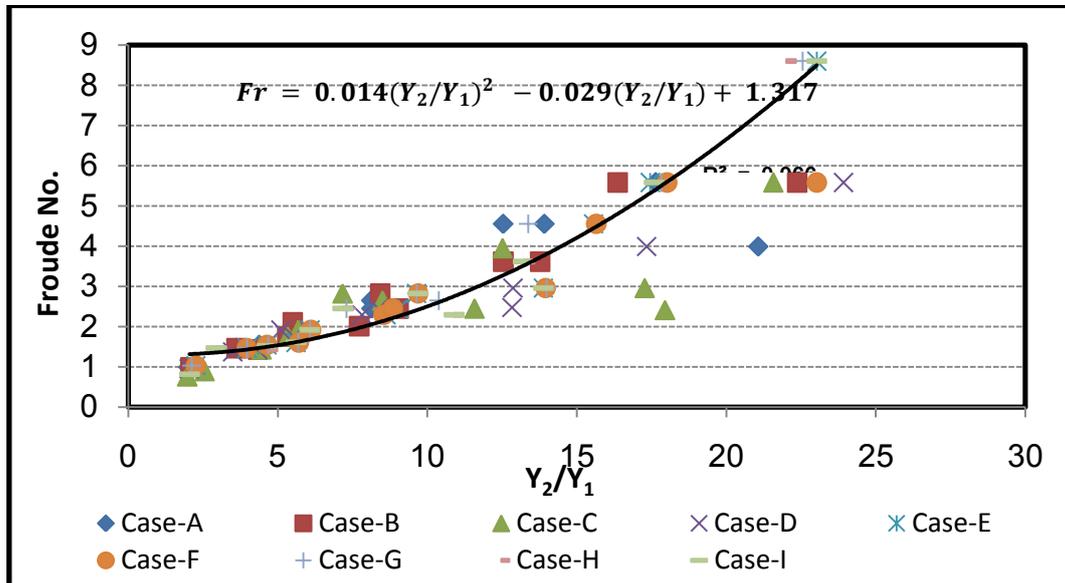
Figure 9: Relationship between Sequent Depth (Y_2/Y_1) and Froude No. (F_r)

4.4. Effect on Hydraulic Jump

The length of the reverse flow "Lrf" over the concrete slab downstream the end step was obtained to get the optimum length of concrete slab. The length of the reverse flow over the concrete slab was measured by using the electromagnetic current-meter. The current-meter recorded the flow velocity at 0.9 of the water depth. The current-meter was moving to the downstream and upstream direction until it gives the zero velocity approximately. Also, the length of the reverse flow was measured by using the steel rod with threat at one of its end. The length of the reverse flow was measured by both of the two methods and compared with the length from the velocity profiles. Fig. (10) shows the distance of reverse flow. These distances are measured during each test.
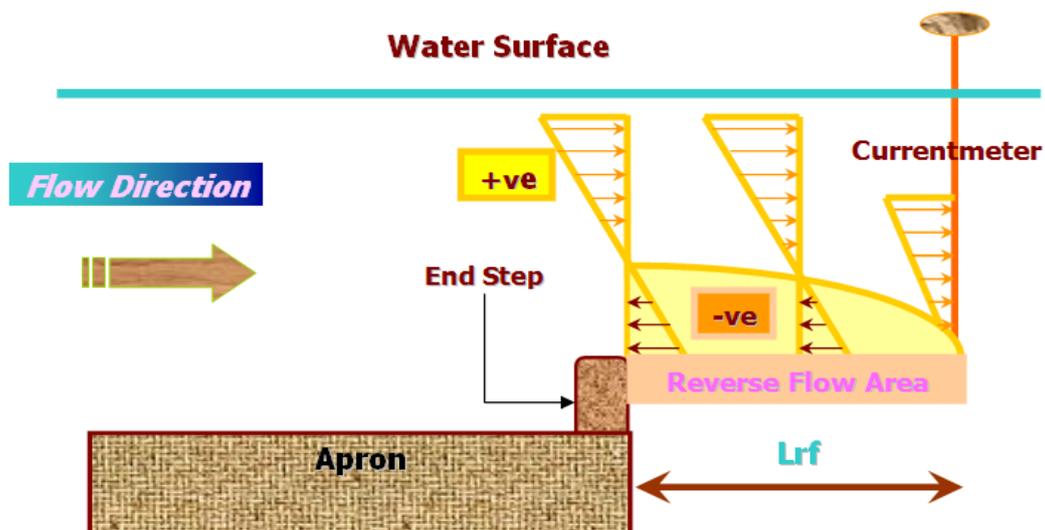
Figure 10: Typical Sketch for the Length of Reverse Flow

During each test series, the hydraulic jump parameters are measured such as the conjugate depth (Y_1), the backup water depth just downstream the gate (Y_3), and the length of the jump (Lsj). Moreover, the gate opening (G.O), the upstream water depth (H_u), and the tail-water depth (Y_t) are measured. The upstream water depth is measured above the sill under the gate to the upstream water level, and the downstream water depth is measured at the end of apron. Fig. (11) illustrates the influence of Relative Length of Jump (L_{sj}/Y_1) on Froude No. (F_r) for all tested cases. From this figure, it is clearly noticed that as the Froude No. increases the relative length of jump increase. For the same Froude No. the maximum value of L_{sj}/Y_1 was found at stilling basin case D. All test gives linear trend with equation $\frac{L_{sj}}{Y_1} = 23.66\,F_r - 9.566$ with R^2=0.94.
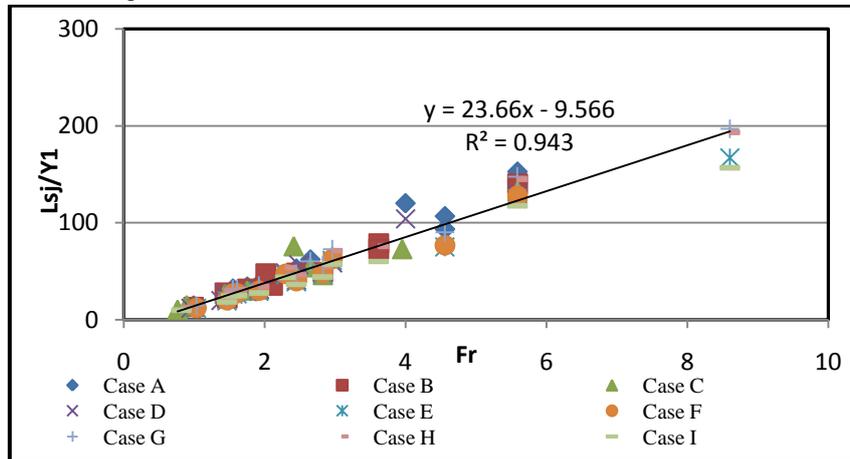
Figure 11: Relationship between Relative Length of Jump (L_{sj}/Y_1) and Froude No. (F_r)

4.5. Velocity Distribution and Velocity Decay over Slab:

The velocity distributions of different locations along the stilling basin were plotted in a dimensionless form (V_b/V_{ave}) by dividing the measured bottom velocity "V_b" at each point depth by "V_{ave}" average velocity. The effect of the geometric shape of each stilling basin for each case was studied in the following sections. Also, the velocity decay near to bed along the stilling basin "V_b" was studied for each test. The relative velocity near the bed "V_b/V_{ave}" versus the relative horizontal distance from the gate "X/L_s" was plotted for different stilling basins. Where: "X" is the horizontal distance, and "L_s" is the length of the concrete slab in Fig. (12). Fig. (12) represents the relation between (X/L) and (V_b/V_{ave}) for test No. 10 (the Discharge=136.1l/sec, Froude number 5.6). All tests showed the same trend for fixed series. The velocity variances between different tests were vanished after X/L_s equal 0.54 except series (F) as the velocity variances were clearly noticed along the tested X/L_s between 0.03-0.54. For the same Froude number the case F gives maximum bed velocity and case D gives the minimum bed velocity.
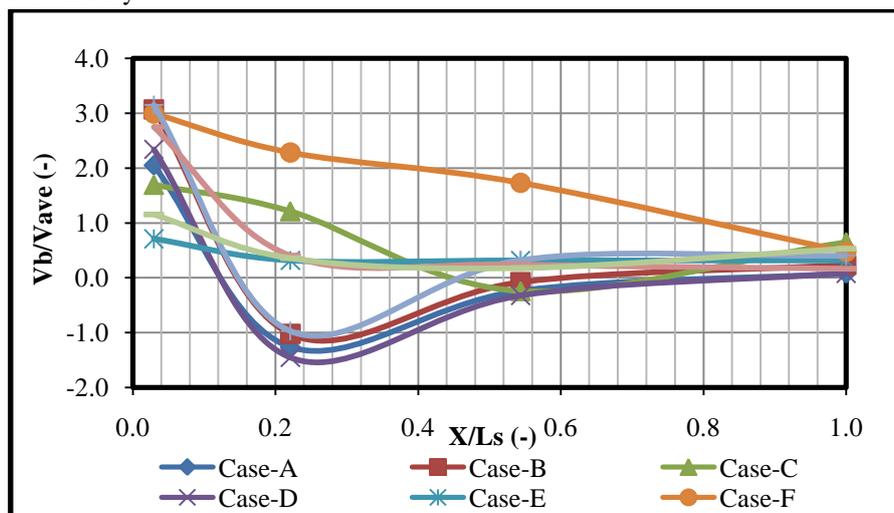
Figure 12: Relationship between X/L_s versus V_b/V_{ave} for test 10

A typical case of velocity profile for different shapes at Fr = 5.6, test 10 is shown in Fig. (13). The x-axis shows the velocities at different relative heights (Y) over the bed, and at nine-sections over the sluiceway apron and beyond it (sec. 1 to sec. 9). The y-axis shows the relative depth of the current-meter, started from the water surface, on the vertical directions (Y = 0.2, 0.4, 0.6, 0.8y). From these profiles, it was found that the wall jet in case of both shapes E, F and GI vanished early before reaching the end of stilling basin (sec. 4), and normal well distribution of the velocity profiles at different sections was obtained compared to the other shapes A, B, C and D. The wall jet of submerged jump may be extended to or beyond the end of apron that means longer lengths of submerged jump will be obtained. Case B creates high values of near bed velocity which are considered as greatly harmful to the movable bed downstream of the regulator stilling basin.
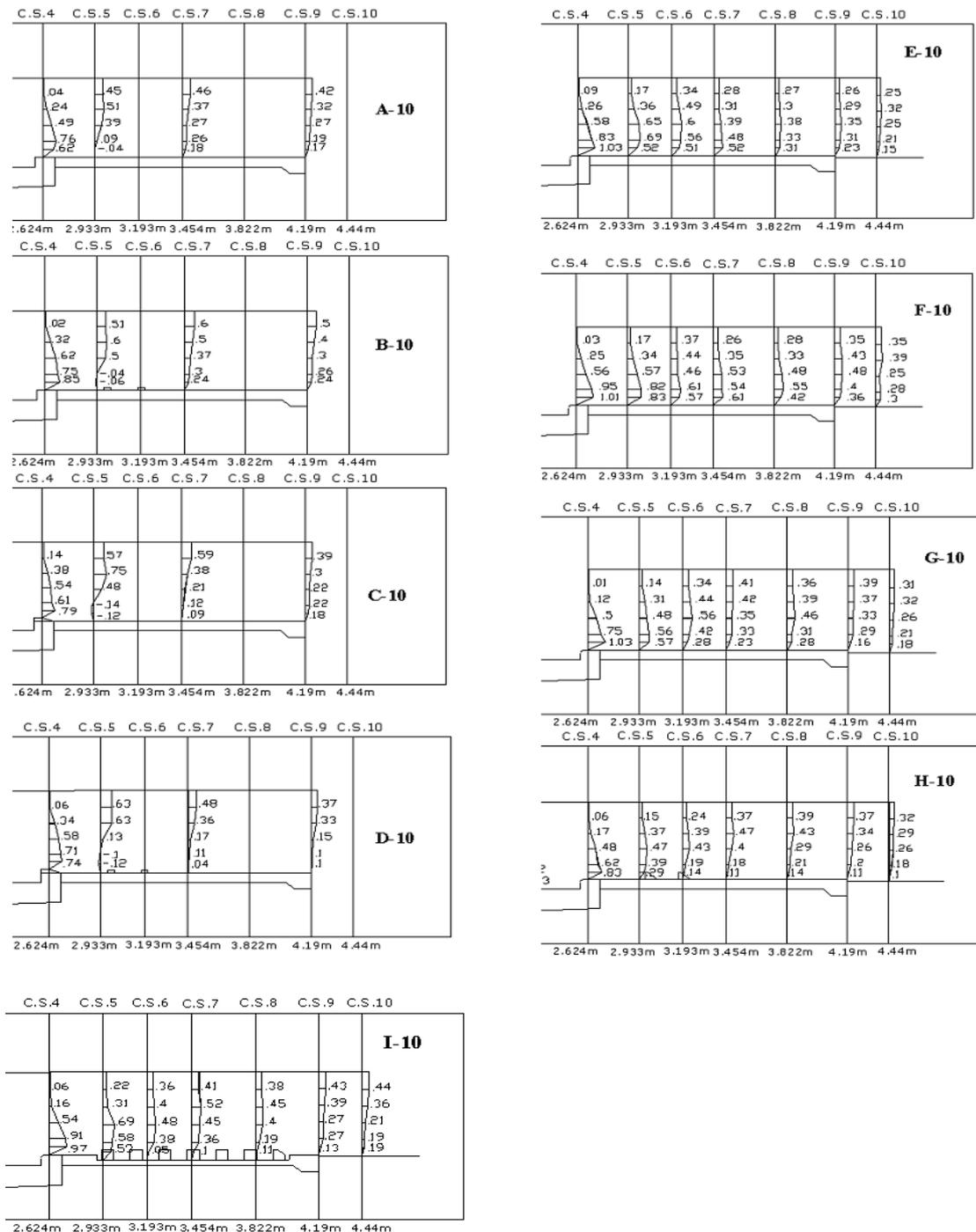
Figure 13: A typical Case of Velocity Profile for Different Shapes

5. Conclusions

Based on the results the following conclusions could be achieved.

- Stilling basin design of curved end step with different radii without baffle blocks and design of curved end step with different shapes and dimension of baffle blocks improves the flow distribution because it vanishes the reverse flow.
- Stilling basin design with curved end step and drop in the slab and seven rows of baffle blocks more safe design for the bed protection.
- Stilling basin desgin with end sill and rounded baffle blocks give maximum relative enregy losses about equal 80%.
- The stilling basins with rounded end step with small radius give maximum value of discharge coefficient (Cd) equal 1.77 which and the stilling basin with additional step on end step give minimum value of (Cd) equal 0.89.
- Stillings basin with rounded end step with two rows of trapezoidal baffle blocks with height equal to its width presents the minimum velocity values for all tested flow conditions compared to other cases.
- The length of the reverse flow near bed over slab "Lrf" that derived from the velocity distribution and measured during runs doesn't reach the end of the slab with all conducted tests.

Notations:

H = Water head above the weir crest [m]
Y_1 = Water depth at the tail gate [m]
Y_2 = The sequent depth
Q = Water discharge through the flume [m3 /s]
g = Gravity acceleration [m/s2]
B = Flume width [m]
V = The mean velocity at the downstream cross section of flume [m/s]
G.O = Gate opening [m]
d50 = Mean particle diameter [m]
Ls = The length of the concrete slab [m]
R = Reynolds number
Fr = Froude number

References

[1]. Chen J. G., Zhang J. M., Xu W. L. and Peng Y. (2014). "Characteristics of the Velocity Distribution in a Hydraulic Jump Stilling Basin with Five Parallel Offset Jets in a Twin-Layer Configuration". Journal of Hydraulic Engineering, Vol. (140), No. (2), pp. 208-217.

[2]. Pagliara S. and Palermo M. (2012). "Effect of Stilling Basin Geometry on the Dissipative Process in the Presence of Block Ramps". Journal Irrigation Drain Engineering, Vol. (138), No. (11), pp. 1027-1031.

[3]. Verma D. and Goel A. (2003). "Development of Efficient Stilling Basins for Pipe Outlets". Journal Irrigation Drain Engineering, Vol. (129), No. (3), pp. 194-200.

[4]. Hossam M. A., Mohamed M. Elgendy, Ahmed. M. H. Mirdan, Abdel Azim A. and Famy .S.F. (2014). "Minimizing Downstream Scour Due to Submerged Hydraulic Ump Using Corrugated Aprons". Ain Shams Engineering Journal, Vol. (5), Issue (4), pp. 1059-1069.

[5]. El-Azab Y. Helal (2014). "Minimizing Scour Downstream of Hydraulic Structures Using Single Line of Floor Water Jets". Ain Shams Engineering Journal, Vol. (5), Issue (1), pp. 17-28.

[6]. Hitham A.S., El-Azab Y. Helal, S.A. Ibrahim and M.F. Sobeih (2012). "Minimizing of Scour Downstream Hydraulic Structures Using Semi-Circular Sill". Menoufia Engineering Journal, Vol. (35), No. (2).

[7]. El-Gamal M. M. (2001). "Effect the Shape of Stilling Basin on Scour Downstream Heading Up Structures", Mansoura Engineering Journal, Vol. (26), No. (2).

[8]. EI Masry A. A., and Sarhan T. H. (2000). "Minimization of Scour Downstream Heading up Structures Using a Single Line of Angle Baffles". Engineering Research Journal, Faculty of Engineering, Helwan University, Mataria, Cairo, Egypt, Vol. (69), pp. 192-207.

[9]. Wafaie and Ehab M. (2001). "Optimum Height for Bed Sills in Stilling basins", and "Optimum Location for Bed Sills in Stilling basins". Bulletin of the Faculty of Engineering, Assiut University, Vol. (29), No. (1), pp. 1-12 and 13-24.

[10]. El Masry, A.A. (2001). "Minimization of Scour Downstream Heading-up Structures Using Double Line of Angle Baffles". Proceedings of Sixth International Water Technology Conference (IWTC), Alexandria, Egypt.

[11]. Ibrahim A.R. (2000). "Analysis and Formulation of Supercritical submerged Flow below Gate in Radial Basin with Lateral Sill", Engineering Research Journal, Faculty of Engineering, Helwan University, Mataria, Cairo, Egypt, Vol. (69), pp. 117-130.

[12]. M.F. Sobeih, E.Y. Helal, T.H. Nassralla, A.A. Abdelaziz (2012). "Scour Depth Downstream Weir with Openings" International Journal Civil Structures Engineering, Vol. (3), No. (1).

[13]. Elsaeed G., Mohamed A., Badawy N., Mohamed A. (2016). "Effect of End Step Shape in the Performance of Stilling Basins Downstream Radial Gates" Journal of Scientific Research & Reports, Vol. (9), No. (1), pp. 1-9, Article No.JSRR.21452.

[14]. Ahmed M. Ibrahem (2014). "Investigating the Design Efficiency of Stilling Basin Downstream Radial Gates", Msc., Benha University, Egypt.